V European Conference on Computational Fluid Dynamics
ECCOMAS CFD 2010
J. C. F. Pereira and A. Sequeira (Eds)
Lisbon, Portugal, 14-17 June 2010

FLOW IN NATURALLY CHANGING CENTRAL AIRWAYS

E. Hylla*, O. Frederich*, F. Thiele*, X. Wang†, I. Wegner†, H.-P. Meinzer†, M. Puderbach¶

*Berlin Institute of Technology, Institute of Fluid Mechanics and Engineering Acoustics
Müller-Breslau-Str. 12, 10623 Berlin, Germany
e-mail: eike.hylla@cfd.tu-berlin.de

†German Cancer Research Center, Department of Medical and Biological Informatics
Im Neuenheimer Feld 280, 69120 Heidelberg, Germany

¶German Cancer Research Center, Department of Radiology
Im Neuenheimer Feld 280, 69120 Heidelberg, Germany

Key words: Bio Fluid Dynamics, Airways, Immersed Boundary Method

Abstract. *To predict and analyze the flow in naturally changing airways several stages of work in different disciplines have to be performed. The CT experiments and image segmentation methods gaining geometries of dynamic airways are presented. The flow simulations within these natural airway geometries were enabled using an Immersed Boundary approach, which is briefly discussed. The focus is set on analyzing and discussing the flow physics in static and dynamic geometries. The results show that the surface deformation has a significant influence on the flow phenomena which should not be neglected for further investigations.*

1 INTRODUCTION

Understanding the flow physics in the upper airways is an important thing e.g. when optimizing the situation for artificially ventilated patients. To achieve that numerical simulations are an essential method to investigate the different physical effects. To gain reliable results realistic airway geometries and boundary conditions are needed. Previously the flow in a static human lung and a Weibel [1] lung model have already been studied in [2] and [3]. Other groups also investigated the flow phenomena in animal, human or models of the lung, e.g. [4]-[7], but none of these considers the motion and deformation of the airways, enforced by the diaphragm. CT experiments are a common way to capture dynamic in vivo airway geometries. To take into account the motion of the bronchial tree, a temporal description of the airways is required, which can be gained by a sequence of CT scans during a breathing cycle. As the level of contamination during the repeating CT scans is too high for humans a pork, with a lung geometry similar to those of a human, is used for the investigations. The CT experiments and the segmentation process require an

cooperation with radiologists and experts in image processing. The automated and well established workflow is presented in detail in [2]. The following section gives an overview over the CT experiments and the segmentation process. Thereafter the numerical methods are presented which enable the flow simulations in complex and moving geometries. The different results for steady and dynamic configurations are discussed in section 5.

2 ACQUISITION OF DYNAMIC AIRWAY GEOMETRIES

2.1 CT experiments

The animal experiment was performed after approval by the local animal experimental committee, and both care and handling of the animal were in accordance with the German law for animal protection. A healthy domestic pig (33 kg) was anesthetized. Mechanical ventilation was performed using intermittent positive pressure ventilation (Evita 4, Draeger, Germany). The respiratory rate was 20 breaths/min with an inspiratory/expiratory ratio of 1:2. A tidal volume (V_t) of 450 ml using a PEEP level of 5 cm H_2O ($\approx$ 490 Pa) was applied. Multislice CT was performed using a 16-detector CT (Aquilion-16, Toshiba, Japan). A charge-coupled device camera was installed on the end of the CT table for chest motion detection. The signal was automatically analyzed using a dedicated software, resulting in a gating signal. Scan parameters were collimation 1 mm, 120 kV, 300 mA, gantry rotation time 0.5 s, pitch 0.15 (helical pitch 2.4), which was adjusted to the breathing rate, small field of view (240 mm), matrix size 512×512, in-plane resolution 0.47×0.47 mm. All volume datasets were reconstructed at 10% increment throughout the respiratory cycle (at 0, 10%, 20%, 30%, 40%, 50%, 60%, 70%, 80%, and 90%) using half-scan reconstruction [8].

2.2 Segmentation

The segmentation of the tracheo-bronchial tree is an important preliminary step for the flow simulation of the airways. According to the complex structure of the bronchial tree with several branching levels, we present a hybrid segmentation method, which is composed of the following four modules: adaptive region growing, boosting, cropping and manual correction (see fig. 1). The algorithm Region Growing [9] is a frequently used technique for segmentation of airways. In this method voxels with gray values within a predefined threshold interval and connected to a seed point are included into the segmentation. Apart from various advantages such as fast runtime and easy usability the main drawback of this method is its sensitivity to leakage. On bronchial tree segmentation leaks occur in the airway wall due to the limited CT resolution and the partial volume effect. Because the airway lumen and the lung interior have similar intensities, the segmentation can be expanded into the lung parenchyma. To avoid this effect we propose an adaptive method [10] in the first module, which performs segmentation in a range of thresholds in a predefined interval simultaneously. After computation, leakage is detected automatically and the threshold before leakage is chosen to be confirmed or adapted by the user.

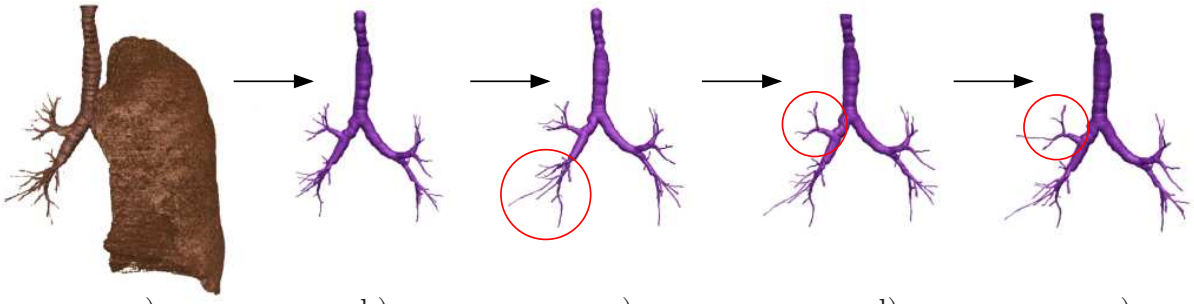

a) b) c) d) e)

Figure 1: Segmentation process: 3d preview a), adaptive region growing b), boosting c), cropping d) and manual correction e).

Because the leakage often occurs in one bronchus only while the growing process could be expanded in all other bronchi, we propose a boosting method [11] in the second module which performs the adaptive region growing method at every leaf of the current bronchial tree. After boosting the segmentation may contain false positive voxels because bronchi seem to end in the lung parenchyma in the CT-images which is due to the partial volume effect. To remove such voxels a cropping method is presented in the third module. Finally the manual correction module offers the user the possibility to process the segmentation using several interactively selected points. All modules are implemented with the open source C++ library Medical Imaging Interaction Toolkit (MITK).

3 NUMERICAL METHODOLOGY

The following investigations are based on the three-dimensional, incompressible Navier-Stokes equations (1) and the law of mass conservation for the incompressible case (2):

$$\frac{\partial \vec{u}}{\partial t} + (\vec{u} \cdot \nabla)\, \vec{u} + \frac{1}{\rho} \nabla p - \nu\, \nabla^2 \vec{u} = 0, \tag{1}$$

$$\nabla \cdot \vec{u} = 0, \tag{2}$$

where $\vec{u}$, p, ρ, ν and t are the velocities, pressure, density, kinematic viscosity and time. The employed flow solver [12] is based on a Finite-Volume discretization of second order accuracy in space and time. The flow variables are calculated successively using the SIMPLE algorithm coupling pressure and velocity fields. A non-body conformal Cartesian discretization is used in which the boundary conditions are imposed by the Immersed Boundary (IB) Method [13].

Immersed Boundary Approach

The capabilities of body conformal discretizations are limited, when it is necessary to represent highly complex and/or moving geometries. The IB Method is an approach,

which is well suited for these applications [14]. It is based on two grids (fig. 2): a Cartesian computational grid (Ω) and a surface grid (Γ_b) representing the boundaries of the fluid

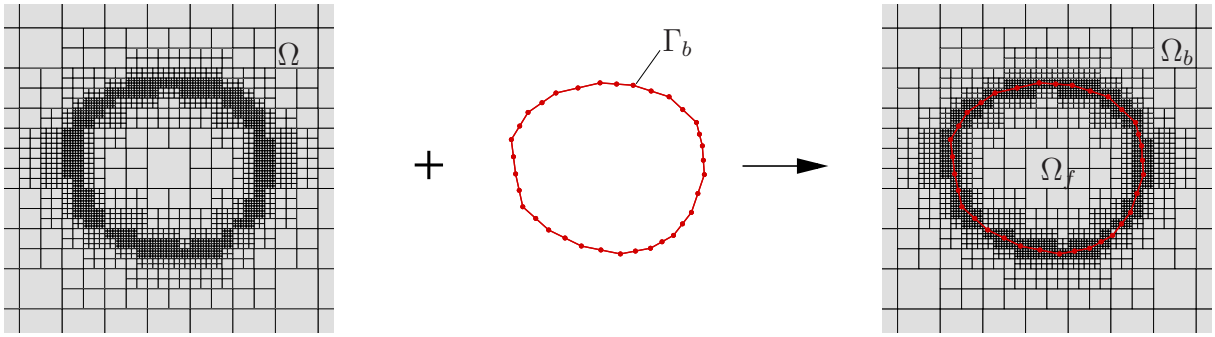

Figure 2: Principle of the IB-method: Ω computational grid (isotropically refined), Γ_b immersed surface grid, non-fluid region Ω_b, fluid region Ω_f.

region. This allows the flow simulation on the Cartesian grid, whereas the boundary conditions are imposed by the *immersed* surface mesh. By replacing the surface during the simulation it is possible to consider moving geometries. There are different ways of imposing the boundary conditions in a IB-method [13]. The current implementation is based on so called *ghost-cells*. Those are cells of the computational domain lying outside but adjacent to the boundary. The ghost-cells are modified in order to fulfill the boundary condition at the IB-surface. To distinguish between fluid (Ω_f) and non-fluid (Ω_b) regions, an identification and marking preprocess has to be performed whenever the surface grid changes. More details about the implementation and validation of the method can be found in [15] and [12].

4 CONFIGURATION AND SETUP

Ten surface configurations (fig. 3 *left* and *middle*) describing the motion of the porcine bronchial tree during one breathing cycle were obtained by the process described in section 2. To generate a higher temporal resolution, additional configurations between the given ones can be interpolated linearly (fig. 3 *middle*). The surface velocity u_{ib} can be approximated with a central difference scheme:

$$\vec{u}_{ib} = \frac{\mathrm{d}\vec{x}}{\mathrm{d}t} \approx \frac{\vec{x}(t+\Delta t) - \vec{x}(t-\Delta t)}{2\Delta t} \,, \tag{3}$$

where $\vec{x}$ is the vector to each point of the surface grid. Currently sinusoidal modulated mass fluxes are defined at the in- and outlets (fig. 3 *right*). The Reynolds number is $\mathrm{Re}_d = 2\,000$ according to the experiments. The computational grid consists of 2 060 993 Cartesian cells and the surface is discretized with 277 632 triangle elements. The computations were performed on 8 CPU's (AMD Opteron 2.2 GHz). The simulation time was $\approx$ 48 h for

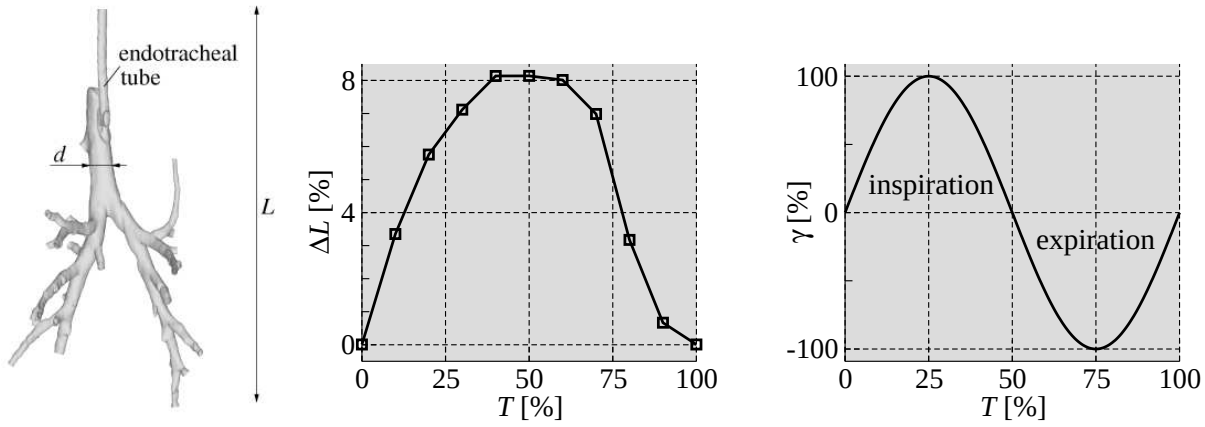

Figure 3: Porcine bronchial tree (*left*) vertical change (*middle*) and generic inlet velocity amplification (*right*) during one breathing cycle.

the steady inspiration case and $\approx 160\,\mathrm{h}$ for one breathing cycle in the dynamic geometry respectively.

5 RESULTS

This section is subdivided into two parts. The first one focuses on the flow phenomena during steady inspiration in a non-moving geometry. The second part discusses the results within the moving geometry. Investigations in a reference geometry of a human lung have shown that the flow can be treated laminar [2].

5.1 Steady inspiration

Following a streamtrace from the inlet to the lowest outlet the absolute velocity, which is dominated by the vertical component w, is decreasing. The most intensive drop of momentum can be found in the upper part, where the fluid has to pass the thin endotracheal tube. Behind the position where the tube enters the trachea ($z/L \approx 0.7$) only a slight pressure drop appears (compare fig. 4 a). Although the Reynolds number is known from the experiment, its influence was studied for the steady case. Fig. 4 b illustrates that the influence is relatively small, which has also been found by Choi et al. [6] in a similar human lung geometry. With an increasing level of bifurcations the absolute velocities are decreasing (fig. 4 c). The upward pointing velocity vectors before the first bifurcation (s_2 and s_3) indicate a recirculation region, induced by the free stream of the endotracheal tube (s_1). Each bifurcation divides the mass flux and as a consequence the mean flow is superposed by secondary flow motion displayed in fig. 4 d.

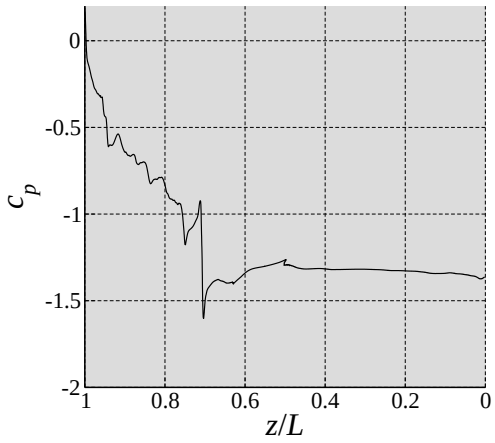

(a) c_p along a streamtrace (Re = 2000).

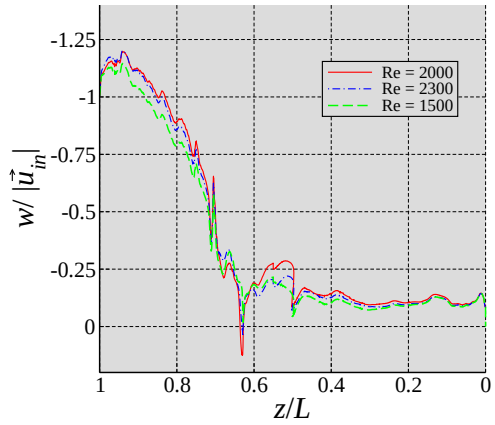

(b) w along a streamtrace.

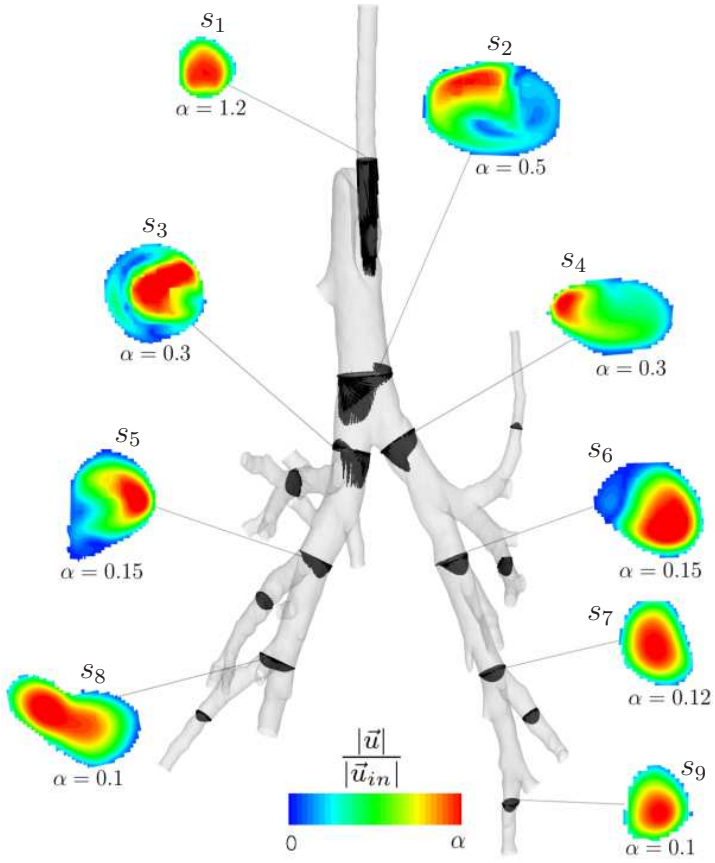

(c) Scaled velocity distributions (Re = 2000).

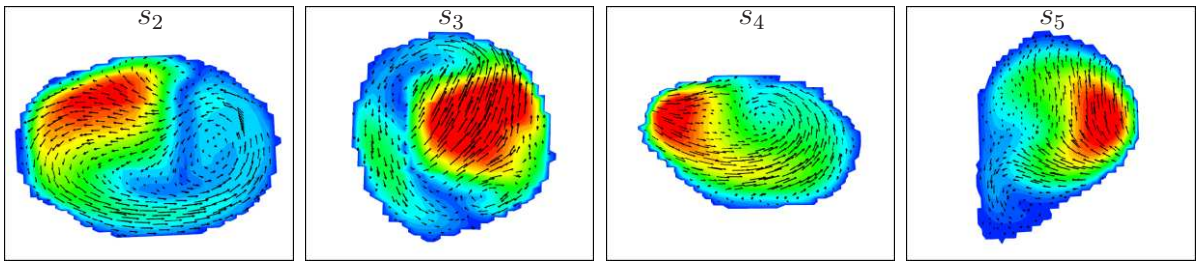

(d) Cross sectional views displaying secondary flow motion for s_2 to s_5.

Figure 4: Results within the static geometry under steady inspiration.

5.2 Dynamic in- and expiration

In the following simulations the inversion of flow direction (inspiration and expiration) and the natural motion of the bronchial tree is considered. Fig. 5 *left* illustrates the maximum intensity of the surface deformation during one breathing cycle. The motion of

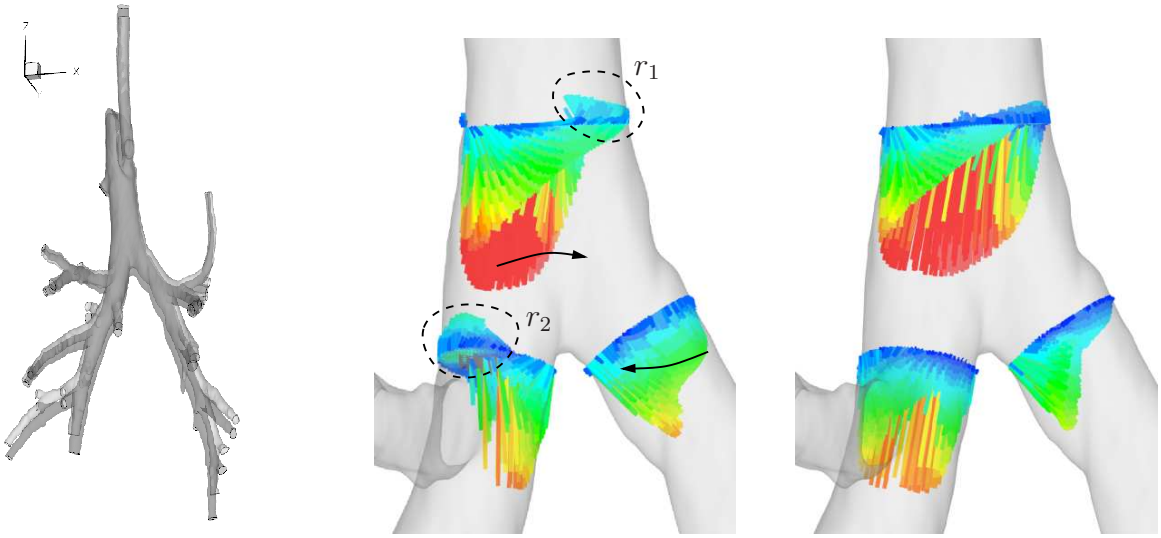

Figure 5: Maximum surface deformations (*left*); velocity profiles at steady inspiration in the static (*middle*) and dynamic geometry (*right*).

the surface has a significant influence on the flow field, proved by the differences in fig. 5 *middle* and *right*. The high velocity values are shifted to the rear center of the trachea and the recirculation region r_1 decreases. In the left daughter branch the recirculation r_2 totally vanishes whereas the velocity profile in the right branch is shifted to the left. Since the bifurcations split the mass fluxes at the inspiration phase, the behavior during expiration is different: In this case two minor streams are joined together into one stream. Fig. 6 shows the velocity distributions (slices s_1 to s_3) at the first bifurcation for one

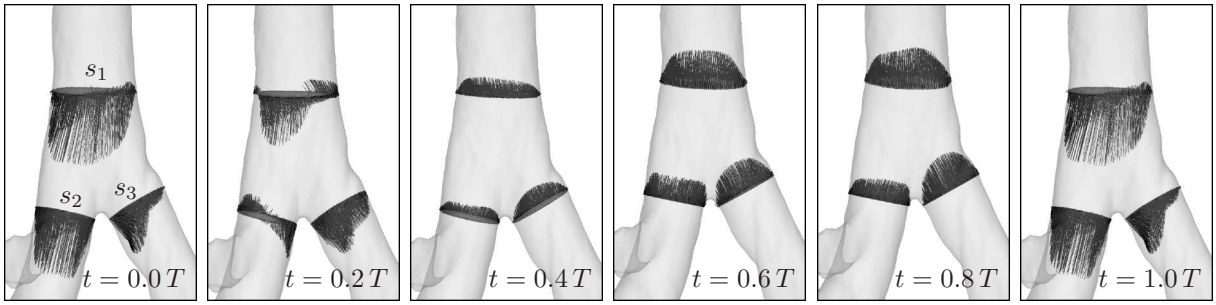

Figure 6: Oscillating flow within the first branching in a dynamic geometry.

breathing cycle. At maximum inspiration ($t = 0$) the flow behavior is similar to the case of steady inspiration in the dynamic geometry (compare fig. 5 *right*). The free stream caused by the endotracheal tube leads the fluid towards the rear center of the trachea. The slice s_1 shows a recirculation region as well. The inversion of flow direction ($t = 0.2\,T$) does not occur simultaneously at the different positions. At expiration ($t = 0.4$ to $0.6\,T$) the velocity distributions are more homogeneous. The longer right main branch is the reason why s_3 shows a typical laminar profile, whereas s_2 has a plateau in its velocity field. Also s_1 shows a slight plateau, which is a common effect, when two or more streams in tubular structures are joining. Thereon the flow direction suddenly reverses to inspiration. Focusing on the first bifurcation in the center of the whole airway geometry, the expiratory phase seems to take longer than the inspiratory. Compared to

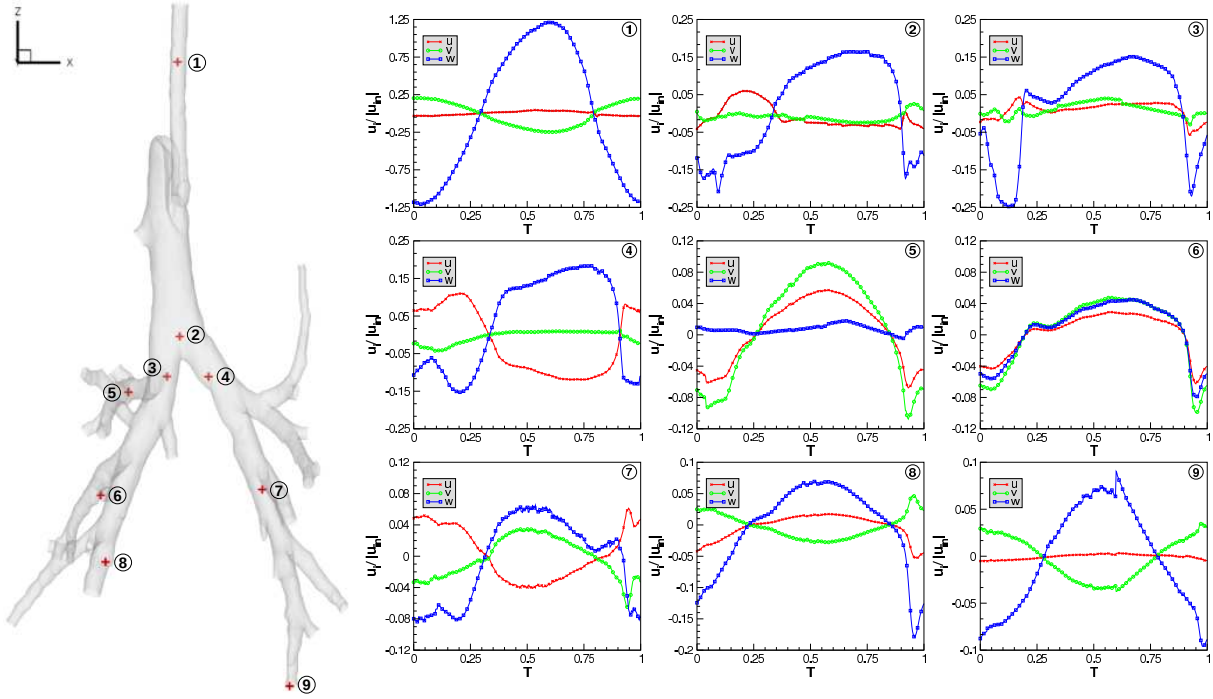

Figure 7: Velocity components u, v and w for selected points over one breathing cycle T starting at maximum inspiration.

the sinusoidal signal at the in- and outlets, the change from expiration back to inspiration ($t = 0.8$ to $1.0\,T$) is delayed. Probably the effect is caused by the constraint of the prescribed surface motion in connection with the fixed mass fluxes at the in- and outlets. The situation may be improved by modeling the neglected lower airways. Fig. 7 depicts the temporal development of velocity components for selected positions. An interpolation of their coordinates in each timestep is necessary due to the motion of the surrounding geometry. As the flow directions in the points usually do not coincide with the coordinate axis (x, y, z) arbitrary contributions of u, v and w appear. The only position where the

monitored signal is similar to sinusoidal signal at the boundary conditions is within the endotracheal tube at point ①. Although ⑧ and ⑨ lie close to the modulated outlets, their temporal history clearly differs from the sinusoidal signal. The long phase of expiration and the sudden change to inspiration can be proved by the time history of ③ and ④ behind the first bifurcation. Values of the helicity ($H = \vec{u} \cdot (\nabla \times \vec{u})$) can be used to indicate rotational secondary flow motion, whereby the sign defines the direction of the rotation. As shown in fig. 8 the rotatory influence during inspiration is more important

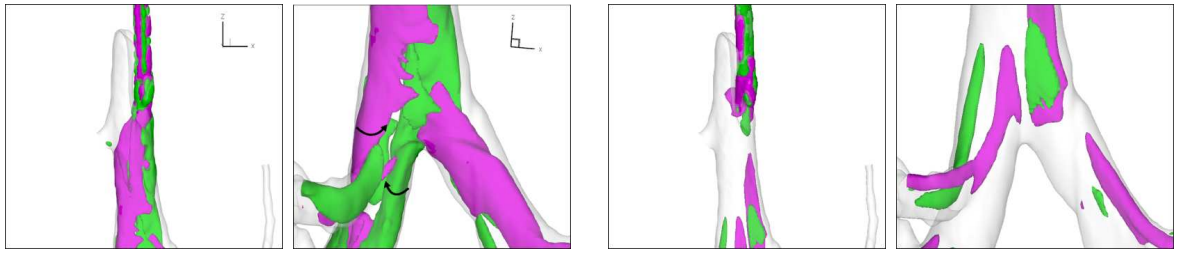

Figure 8: Iso surfaces displaying positive (green) and negative (purple) helicity values at maximum inspiration (*left*) and expiration (*right*).

than during the expiration phase. Depending on the flow direction the bifurcations divide or join the mass fluxes, which appears to be the reason for the different helicity intensities. These counter rotating vortex pairs have also been found in human airways [2].

6 CONCLUSIONS

To analyze the flow physics in naturally changing central airways their geometries and deformations have to be extracted. The CT experiments and the image processing is done by experts in radiology and medical informatics. A self-developed methodology on the base of the Immersed Boundary method enables dynamic flow simulations. Steady simulations show a negligible influence of the Reynolds number at about Re= 2000. The necessity of considering the motion of the geometry is proved by steady inspiration in a moving geometry. The oscillating flow field in the dynamic geometry shows some kind of delayed reaction to the change from ex- to inspiration, which has to be examined further. Thereafter different ventilation strategies can be discussed in the future. The segmentation method including the boost algorithm allows an increase of the segmentation depth. Flow simulations within these more realistic geometries will be performed and offer extensive details of the flow physics in higher level branches. The generically modulated mass flow at the tubular inflow will be replaced by experimental data, gained during the CT scans.

7 ACKNOWLEDGMENTS

The financial support of the German Research Foundation (DFG) within the scope of the research project “Protective Artificial Respiration” is gratefully acknowledged.

REFERENCES

[1] Weibel, E. R.: Morphometry of the human lung, Springer, Berlin (1963).

[2] Frederich, O., Amtsfeld, P., Hylla, E., Thiele, F., Puderbach, M., Kauczor, H.-U., Wegner, I., Meinzer, H.-P.: Numerical Simulation and Analysis of the Flow in Central Airways. STAB 2008, *Notes on Numerical Fluid Mechanics and Multidisciplinary Design VII*, **Vol. 112** (in press).

[3] Frederich, O., Hylla, E., Amtsfeld, P., Thiele, F., Puderbach, M., Kauczor, H.-U., Wegner, I., and Meinzer, H.-P.: Numerically Predicted Flow in Central Airways: Modelling, Simulation and Initial Analysis. *In: Proceedings of 6th Int. Symposium Turbulence and Shear Flow Phenomena*, Seoul (2009).

[4] Nowak, N., Kakade, P. P. and Annapragada, A. V.: Computational Fluid Dynamics Simulation of Airflow and Aerosol Deposition in Human Lungs. *Annals of Biomedical Engineering*, **Vol. 31**, pp. 374–390 (2003).

[5] Kabilan, S., Lin, C.-L. and Hoffman, E. A.: Characteristics of airflow in a CT-based ovine lung: a numerical study. *J Appl Physiol*, **Vol. 102**, pp. 1469–1482 (2007).

[6] Choi, J., Tawhai, M. H., Hoffman, E. A. and Lin, C.-L.: On intra- and intersubject variabilities of airflow in the human lungs. *Physics of Fluids*, **Vol. 21**, 101901 (2009).

[7] Kleinstreuer, C. and Zhan, Z.: Airflow and Particle Transport in the Human Respiratory System. *Annual Review of Fluid Mechanics*, **Vol. 42**, pp. 301-334 (2010).

[8] Zaporozhan, J., Ley, S., Unterhinninghofen, R., Saito, Y., Fabel-Schulte, M., Keller, S., Szabo, G. and Kauczor, H.-U.: Free-breathing threedimensional computed tomography of the lung using prospective respiratory gating: charge-coupled device camera and laser sensor device in an animal experiment. *Invest Radiol.* **Vol. 41**, pp. 468–475 (2006).

[9] Adams, R. and Bischof, L.: Seeded region Growing. *IEEE Transactions on Pattern Analysis and Machine Intelligence*, **Vol. 16**, no. 6, pp. 641–647 (1994).

[10] Wolber, P., Wegner, I., Heimann, T., Wolf, I. and Meinzer, H.-P., Tracking und Segmentierung baumförmiger, tubulärer Strukturen mit einem hybriden Verfahren. *Bildverarbeitung für die Medizin*, pp. 242–246 (2008).

[11] Gergel, I., Wegner, I., Tetzlaff, R. and Meinzer, H.-P.: Zweistufige Segmentierung des Tracheobronchialbaums mittels iterativen adaptiven Bereichswachstumsverfahren. *Bildverarbeitung für die Medizin*, pp. 56–60 (2009).

[12] Hylla, E., Frederich, O., Mauß, J. and Thiele, F.: Application of the immersed boundary method for the simulation of incompressible flows in complex and moving geometries, STAB 2008, *In: Notes on Numerical Fluid Mechanics and Multidisciplinary Design VII*, **Vol. 112** (in press).

[13] Mittal, R. and Iaccarino, G.: Immersed boundary methods, *Annual Review of Fluid Mechanics*, **Vol. 37**, pp. 239–26 (2005).

[14] Tseng,Y.H., Ferziger, J. H., A ghost-cell immersed boundary method for flow in complex geometry, *Journal of Computational Physics*, **Vol. 192**, pp. 593–623 (2003).

[15] Hylla, E., Validierung und Erweiterung eines numerischen Verfahrens zur Simulation von inkompressiblen Strömungen mittels der Immersed Boundary Methode, *Diploma thesis*, ISTA, TU Berlin (2008).